

On the hard γ -ray spectrum of the supernova remnant G106.3+2.7

YIWEI BAO¹ AND YANG CHEN^{1,2}

¹*Department of Astronomy, Nanjing University, 163 Xianlin Avenue, Nanjing 210023, China*

²*Key Laboratory of Modern Astronomy and Astrophysics, Nanjing University, Ministry of Education, Nanjing, China*

(Received; Revised; Accepted)

Submitted to ApJL

ABSTRACT

Tibet AS γ experiment has measured γ -ray flux of supernova remnant G106.3+2.7 up to 100 TeV, suggesting it to be potentially a “PeVatron”. Challenge arises when the hadronic scenario requires a hard proton spectrum (with spectral index ≈ 1.8), while the diffusive shock acceleration can only predict a soft (with spectral index ≥ 2) proton spectrum. In this paper, we explore an alternative scenario to explain the γ -ray spectrum of G106.3+2.7 within the current understanding of acceleration and escape processes. We consider that the cosmic rays upstream of the shock are scattered by the turbulence driven via Bell instability. The resulting hadronic γ -ray spectrum is novel, dominating the contribution to the emission above 10 TeV, and can explain the bizarre broadband spectrum of G106.3+2.7 in combination with leptonic emission from the supernova remnant.

Keywords: ISM: supernova remnants — ISM: individual objects (G106.3+2.7) — diffusion — (ISM:) cosmic rays

1. INTRODUCTION

Galactic cosmic rays (GCRs) are mostly charged particles (mainly protons) with energy up to the “knee” (~ 1 PeV). Based on energetic arguments, supernova remnants (SNRs) are usually believed to be the accelerators of GCRs. However, although a large number of SNRs have been detected in γ -rays, none of these SNRs has been confirmed to be a PeV particle accelerator, as called “PeVatron” (see e.g., [Bell et al. 2013](#)). Discovered in the DRAO Galactic-plane survey ([Joncas & Higgs 1990](#)), G106.3+2.7 is an cometary SNR with a tail in the southwest and a compact head (containing PSR J2229+6114) in the northeast. Recently, HAWC and AS γ experiments have reported the γ -ray spectrum of SNR G106.3+2.7 above 40 TeV, arguing that SNR G106.3+2.7 (at a distance of 800 pc away from Earth, [Kothes et al. 2001](#)) is a promising PeVatron candidate ([Albert et al. 2020](#); [Amenomori et al. 2021](#)). In particular, [Amenomori et al. \(2021\)](#) for the first time measured the γ -

ray flux up to 100 TeV, finding that the centroid of γ -ray emissions is away from PSR J2229+6114 by 0.44° (~ 6 pc at a distance of 800 pc), and is well correlated with a molecular cloud (MC), implying that the high-energy γ -rays can be of hadronic origins.

Both leptonic and hadronic models have been proposed to give a plausible explanation to the spectral energy distribution (SED) of the SNR. In the leptonic scenario, the electrons are suggested to be transported to its current position from the pulsar wind nebula (PWN, Amenomori et al. 2021; Liu et al. 2020), or be accelerated by the SNR shock directly (Amenomori et al. 2021); in the hadronic scenario, the protons are suggested to be accelerated by the SNR shock in earlier ages, or re-accelerated by the PWN adiabatically (Amenomori et al. 2021). In order to figure out the origin of γ -rays, Ge et al. (2020) separate the PWN-dominated X-ray emitting region in the northeast from the other (southwestern) part of the SNR using XMM-Newton and Suzaku observations. They found that a pure leptonic model can hardly fit the X-ray and γ -ray spectral data of the latter part of SNR simultaneously. Therefore the SED can only be explained with a hadronic (with a proton spectral index ≈ 1.8 , Amenomori et al. 2021) or a hybrid leptonic-hadronic (with a proton index ≈ 1.5 , Ge et al. 2020) model. However, challenge arises when hard proton spectrum is required in both hadronic and hybrid leptonic-hadronic models, while numerical simulations show that diffusive shock acceleration can only give rise to a soft proton spectrum (with spectral index ≥ 2 , see e.g., Caprioli et al. 2020).

Amenomori et al. (2021) suggest that the very hard proton spectrum can be obtained in very efficient acceleration (which seems to be an extreme case), and after a very slow particle diffusion. We here explore an alternative self-consistent scenario in which the γ -ray spectrum can be explained more naturally. The magnetic field in the upstream of the SNR shock is believed to be amplified via the non-resonant Bell instability (Bell 2004; Amato & Blasi 2009): protons escaping from the upstream of the shock can drive non-resonant turbulence whose scale is smaller than the Larmor radius of the escaped particles, and the relatively-low-energy particles are thus diffused by the magnetic field amplified by the non-resonant turbulence (for reviews, see e.g., Blasi 2013). Based on the numerical simulations (Bell 2004; Bell et al. 2013), we calculate the escape process from the first principle instead of a model with apriori phenomenological assumptions. The resulting proton spectrum is novel and can explain the hard γ -ray spectrum well. The model is described in §2 and the SED of the SNR G106.3+2.7 is fitted in §3, discussion is presented in §4 and the conclusion is drawn in §5.

2. MODEL DESCRIPTION

For simplicity, we follow the approximation that the global maximum energy is reached at the beginning of the Sedov phase in which $R_{\text{sh}} \propto t^{2/5}$ (see e.g., Ohira et al. 2012). We use the canonical diffusive shock acceleration scenario in which the spectrum of accelerated particles $f_{\text{acc}} \propto E^{-2}$. The maximum proton energy can be given by (Bell et al. 2013)

$$E_{\text{max}}(t) = 230 n_e^{1/2} \left(\frac{\eta}{0.03} \right) \left(\frac{v_{\text{sh}}}{10^4 \text{kms}^{-1}} \right)^2 \left(\frac{R_{\text{sh}}}{\text{pc}} \right) \text{TeV}, \quad (1)$$

where η is the acceleration efficiency, n_e the electron number density of the interstellar medium (ISM), v_{sh} the velocity of the shock, and R_{sh} the radius of the shock.

Following Cardillo et al. (2015), we calculate the spectrum of escaped protons in the Sedov phase. In the upstream, the protons are scattered by the wave generated via escaping of higher-energy protons, and therefore there is no wave upstream to scatter the protons with the highest-energy

$E_{\max}(t)$ (Bell 2004; Bell et al. 2013). Hence, the latter escape the system quasi-ballistically at a speed $\sim c$, inducing a current $j_{\text{CR}} = ev_{\text{sh}}\pi p_{\text{max}}^3 f_0(p_{\text{max}})$ at the shock, where f_0 is the isotropic part of cosmic ray (CR) distribution function in momentum space at the shock, and p_{max} the maximum momentum of the non-thermal protons (Bell et al. 2013). On the other hand, the CR pressure at the shock (Bell et al. 2013)

$$P_{\text{CR}} = \frac{4\pi}{3} c p_{\text{max}}^4 f_0(p_{\text{max}}) \ln \left(\frac{p_{\text{max}}}{p_0} \right), \quad (2)$$

where p_0 is the minimum momentum of non-thermal protons. Following Bell et al. (2013), we assume that the CR pressure is a fixed ratio of the ram pressure ρv_{sh}^2 (where ρ is the mass density of the preshock ISM), so j_{CR} can be calculated to be (the coefficient is a constant which is not important in the calculation)

$$j_{\text{CR}} \propto \frac{e\rho v_{\text{sh}}^3}{E_{\max} \ln(E_{\max}/E_0)}, \quad (3)$$

where E_{\max} and E_0 are maximum and minimum energies of protons, respectively.

The total number of the escaped protons with energy $E_{\max}(t)$ can thus be evaluated via

$$eN_{\text{esc}}(E_{\max}) dE_{\max} = 4\pi R_{\text{sh}}^2 j_{\text{CR}} dt. \quad (4)$$

So it can be expressed as (see Cardillo et al. 2015, for derivation)

$$N_{\text{esc}}(E_{\max}) \propto \rho v_{\text{sh}}^2 R_{\text{sh}}^3 E_{\max}^{-2} \left[\frac{1 + \ln(E_{\max}/E_0)}{\ln(E_{\max}/E_0)^2} \right]. \quad (5)$$

3. APPLICATION TO SNR G106.3+2.7

To characterize the γ -ray radiation from SNR G106.3+2.7, we consider a truncated molecular cloud cone subtending solid angle Ω at the SNR with inner radius R_1 and outer radius R_2 . and The diffusion coefficient near the SNR is adopted to be $D(E) = D_{\text{ISM}}/K_{\text{sl}}$, where $D_{\text{ISM}} = 4.16 \times 10^{28} (E/4 \text{ GeV})^{0.5} \text{ cm}^2 \text{ s}^{-1}$ (Yuan et al. 2017, model DR2), and K_{sl} is the modification factor.

The diffusion equation for protons with energy E escaping the shock when the shock radius was R_{sh} at time T_{esc} writes

$$\frac{\partial}{\partial t} f(E, r, t) = \frac{D(E)}{r^2} \frac{\partial}{\partial r} \left[r^2 \frac{\partial}{\partial r} f(E, r, t) \right] + Q, \quad (6)$$

where

$$Q = \frac{N_{\text{esc}}(E)}{4\pi R_{\text{sh}}^2} \delta(r - R_{\text{sh}}) \delta(t - T_{\text{esc}}) = \frac{C_Q \rho v_{\text{sh}}^2 R_{\text{sh}}^3 E_{\max}^{-2}}{4\pi R_{\text{sh}}^2} \left[\frac{1 + \ln(E_{\max}/E_0)}{\ln(E_{\max}/E_0)^2} \right] \delta(r - R_{\text{sh}}) \delta(t - T_{\text{esc}}), \quad (7)$$

with C_Q a constant to be considered later.

Defining a new function $F = Rf(E, r, t)$, Equation 6 reads

$$\frac{\partial}{\partial t} F = D(E) \frac{\partial^2 F}{\partial r^2} + Q(E, r, t)r \quad (8)$$

According to Atoyan et al. (1995), the Green function for the Equation 8 is

$$G(E, r, t; \xi, T_{\text{esc}}) = \frac{1}{\sqrt{\pi} R_{\text{dif}}} \left\{ \exp \left[- \left(\frac{r - \xi}{R_{\text{dif}}} \right)^2 \right] - \exp \left[- \left(\frac{r + \xi}{R_{\text{dif}}} \right)^2 \right] \right\}, \quad (9)$$

where $R_{\text{dif}} = 2\sqrt{D(E)(t - T_{\text{esc}})}$ is the diffusion length scale. The solution of Equation 6 is thus

$$f(E, r, t) = \frac{1}{r} \int_0^\infty Q(r - \xi)(r - \xi)G(E, r, t; R_{\text{sh}}, T_{\text{esc}})d\xi. \quad (10)$$

At time T_{age} , the differential number of protons with energy E lying inside the concentric spherical molecular cloud shell can thus be calculated to be

$$N_{\text{CR,MC}} = \int_{R_1}^{R_2} f(E, r, t)\Omega r^2 dr. \quad (11)$$

Finally the γ -ray luminosity is evaluated via the cross-section presented in Kamae et al. (2006). In addition to the hadronic component, we also add a leptonic component contributed by the electrons accelerated by the SNR shock. The electron spectrum is constrained by the radio (dominated by the SNR Pineault & Joncas 2000) and X-ray (Ge et al. 2020; Fujita et al. 2021)¹ radiations. We approximate electron spectrum to be a broken power-law

$$\frac{dN_e}{dE} \propto \begin{cases} E^{-\alpha_1} & E \leq E_b \\ E^{-\alpha_2} & E_b < E < E_{\text{max,global}}. \end{cases} \quad (12)$$

We fit the SED as is plotted in Figure 1, with the parameters listed in Table 1, where R_{now} is the radius of the SNR at present, E_{SN} the explosion energy of the SNR, M_{ej} the ejecta mass, B the magnetic field strength, and W_e the total electron energy. T_{CMB} , T_{FIR} , and T_{NIR} are the temperatures of the CMB, far infrared, and near infrared photons, respectively; u_{CMB} , u_{FIR} , and u_{NIR} are energy densities of the CMB, far infrared, and near infrared photons, respectively. We find that the parameters are insensitive to X-ray flux, since we can fit the X-ray data from Ge et al. (2020) and Fujita et al. (2021) with very similar parameters.

Since the hadronic γ -ray luminosity $L_{\text{pp}} \propto \Omega n_{\text{MC}}$ (where n_{MC} is the number density of the MC, a free parameter), and $L_{\text{pp}} \propto E_{\text{esc}} \propto C_Q$, $L_{\text{pp}} \propto C_Q n_{\text{MC}} \Omega$. Therefore, we only list $C_Q n_{\text{MC}} (\Omega/4\pi)$ as a single parameter in Table 1. At each time t , the protons with energy less than $E_{\text{max}}(t)$ are trapped by the turbulence driven by the escaping protons with energy $E_{\text{max}}(t)$ via Bell instability. At present, protons with energy $\lesssim 58$ TeV are still trapped by the turbulence. Therefore the non-thermal proton spectrum in the MC is almost a δ function, leading to a novel hadronic γ -ray spectrum. Dominating the γ -ray flux in $\lesssim 500$ GeV, the leptonic component (the cyan line in Figure 1) is consistent with the Fermi observations (Xin et al. 2019) and X-ray observations (Ge et al. 2020; Fujita et al. 2021). Meanwhile, the hadronic γ -ray radiation contributed by pp interactions (the yellow line) has a very hard spectrum ($dN/dE \propto E^{-1}$) in $\lesssim 500$ GeV. The spectrum above 10 TeV is dominated by the hadronic component, and the whole γ -ray spectrum can be explained by the hybrid model naturally.

4. DISCUSSION

There remains some uncertainty about the age of the SNR: although the characteristic age of PSR J2229+6114 ($\approx 10^4$ yr) is usually adopted to be the age of the SNR, sometimes the SNR is suggested to be very young (~ 1 kyr, see e.g., Albert et al. 2020). With an adiabatic model

¹ The former X-ray flux is extracted from the region essentially overlapping the molecular cloud, and the latter flux from the regions covering most of the SNR

($R_{\text{sh}} \approx 1.2(E_{\text{SN}}/\rho_{\text{ISM}})^{1/5}t^{2/5}$, where ρ_{ISM} is the density of the ISM), [Kotthes et al. \(2001\)](#) estimated that $E_{\text{SN}} \approx 7 \times 10^{49}$ if the age of the SNR were ≈ 10 kyr. However, as is estimated in [Cardillo et al. \(2015\)](#), [Equation 1](#) indicates that the global maximum energy $E_{\text{max,global}} \propto E_{\text{SN}}$, and SNRs with low E_{SN} can hardly accelerate CRs to $\sim 10^2$ TeV. Although the dilemma may be solved with asymmetry incorporated, in this paper we consider a spherically symmetric scenario in which $E_{\text{SN}} = 10^{51}$ erg (the canonical value) and $T_{\text{age}} = 1000$ yr. Assuming a canonical braking index $n = 3$, the real age of the pulsar writes $T_{\text{age}} = \tau_c[1 - (P_0/P_{\text{now}})^2]$, where τ_c is the characteristic age of the pulsar, P_0 the initial spin period of the pulsar, and P_{now} the spin period of the pulsar at present. For PSR J2229+6114, $P_{\text{now}} = 50$ ms ([Halpern et al. 2001](#)), and T_{age} can be as small as ~ 1 kyr if P_0 is close to P_{now} . The P_0 assumed here is possible since in pulsar evolution models, P_0 is usually suggested to be in a wide range from ~ 4 ms to ~ 400 ms (see e.g., [Arzoumanian et al. 2002](#); [Faucher-Giguère & Kaspi 2006](#); [Popov et al. 2010](#)). Instances in which $P_0 \approx P_{\text{now}}$ and $T_{\text{age}} \ll \tau_c$ can also be found in the catalog: (a) CCO 1E 1207.4–5209 inside SNR G296.5+10.0 has $P_0 \approx P_{\text{now}} = 424$ ms, leading to $\tau_c > 27$ Myr, which exceeds the age of the SNR by 3 orders of magnitude ([Gotthelf & Halpern 2007](#)), and (b) PSR J1852–0040 is suggested to have $P_0 \approx P_{\text{now}} \approx 10^2$ ms, giving rise to $\tau_c \approx 2 \times 10^8$ yr, 4 orders of magnitude larger than $T_{\text{age}} \sim 5 \times 10^3$ yr measured from the observation on its associated SNR ([Gotthelf et al. 2005](#)).

On the other hand, as can be seen from [Equation 1](#), E_{max} is determined by the R_{sh} and v_{sh} which can be constrained by observations directly, irrespective of T_{age} : [Ge et al. \(2020\)](#) showed that v_{sh} is at least 3000 km s^{-1} in the southwest region based on the absence of thermal X-ray emissions, while $R_{\text{sh}} \approx 6$ pc can be estimated via radio observations (see e.g., [Amenomori et al. 2021](#), for the multi-wave length morphology). Although T_{age} does affect R_{dif} , its impacts can be compensated by K_{sl} which is a free parameter. Hence, for simplicity we only consider a spherically symmetric SNR evolving following the well-known model² ([Truelove & McKee 1999](#)).

Our particle escaping scenario has an interesting characteristic: in a spherically symmetric system, there will be a sharp cutoff in the γ -ray spectrum. Meanwhile, smoother break can be predicted if asymmetric morphology is taken into account: asymmetric shock velocity distribution gives rise to asymmetric $E_{\text{max,global}}$ distribution, and an integration over the whole SNR consequently smoothen the sharp cutoff, leading to a break in the γ -ray spectrum. The escape scenario presented in this paper can coexist with the former continuous escape scenarios. During the lifetime of SNR, the shock may break and the CRs can thus escape with continuous power-law spectra, which is the case as previously adopted (see e.g., [Li & Chen 2010](#); [Ohira et al. 2011](#)). In the SNR catalog³ ([Ferrand & Safi-Harb 2012](#)), there are only a few SNRs with γ -ray emissions in $\lesssim 10$ TeV are confirmed to be of hadronic origin, and our novel hadronic spectrum may be found in more SNRs with the help of LHASSO, AS γ and HAWC experiments in future.

5. CONCLUSION

In this paper, we explore an alternative plausible scenario to explain the bizarre γ -ray spectrum of SNR G106.3+2.7 within the current acceleration theory. Apart from the common leptonic component which can be constrained by radio and X-ray observation, we add a novel hadronic component. The hadronic component arises from the escape scenario proposed by [Bell \(2004\)](#) and [Cardillo et al.](#)

² See [Leahy & Williams \(2017\)](#) for a fast python calculator on SNR evolution

³ <http://snrcat.physics.umanitoba.ca/SNRtable.php>

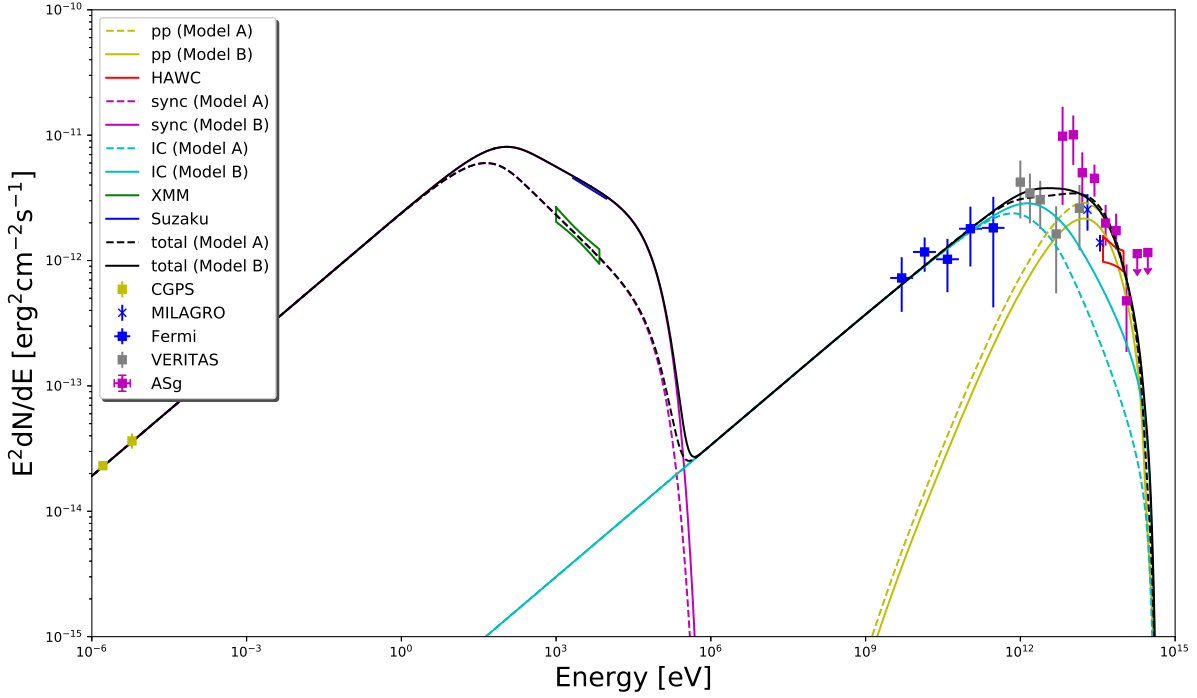


Figure 1. SED of the emission from SNR G106.3+2.7. The CGPS data are taken from Pineault & Joncas (2000), XMM-Newton data from Ge et al. (2020), Suzaku data from Fujita et al. (2021), Fermi-LAT data from Xin et al. (2019), VERITAS data from Albert et al. (2020), HAWC data from Albert et al. (2020), and AS γ data from Amenomori et al. (2021).

(2015), in which the CRs at the shock are diffused by turbulence generated by higher energy CRs escaping upstream. Consequently, at time t , only CRs with energy $E_{\max}(t)$ can escape upstream, while CRs with lower energy are confined. The resulting hadronic spectrum is quite hard, and can explain the bizarre γ -ray spectrum of SED of SNR G106.3+2.7 well.

As can be seen from our calculation, although SNR G106.3+2.7 is sometimes explained as a “PeVatron”, current theory can also give rise to a hard γ -ray spectrum extending to 100 TeV with $E_{\max, \text{global}} \approx 4 \times 10^2$ TeV. Hence detection of 100 TeV γ -ray emissions is a necessary condition for “PeVatron” rather than a sufficient condition. More observations are required to confirm whether G106.3+2.7 is a “PeVatron” or not.

We are in debt to Pasquale Blasi for fruitful discussion, Yutaka Fujita, Ruo-Yu Liu, Qiang Yuan and Xiangdong Li for helpful comments. This work is supported by the National Key R&D Program of China under grants 2017YFA0402600, NSFC under grants 11773014, 11633007, 11851305 and U1931204.

Table 1. Fitting Parameters

Parameter	Model A	Model B
T_{age} (yr)	1000	...
R_{now} (pc)	5.24	...
$E_{\text{max,global}}$ (TeV)	427	...
E_0 (GeV)	1.0	...
R_1 (pc)	7	...
R_2 (pc)	10	...
E_{SN} (erg)	10^{51}	...
d (pc)	800	...
M_{ej} (M_{\odot})	1.0	...
n_{e} (cm^{-3})	0.6	...
η	0.06	...
$n_{\text{MC}}C_{\text{Q}} (\Omega/4\pi)$ ($\text{erg cm}^{-3} \text{s}^{-1}$)	8×10^{-43}	6×10^{-43}
K_{sl}	100	...
E_{b} (TeV)	12	16.5
α_1	2.3	...
α_2	3.8	3.45
B (μG)	4.6	...
W_{e} (erg)	6.8×10^{47}	...
T_{CMB} (K)	2.73	...
u_{CMB} (eV cm^{-3})	0.25	...
T_{FIR} (K)	25	...
u_{FIR} (eV cm^{-3})	0.2	...
T_{OPT} (K)	3000	...
u_{OPT} (eV cm^{-3})	0.3	...

REFERENCES

- Amenomori, M., Bao, Y.W. et al. (Tibet ASg collaboration) 2021, Nat Astron doi:10.1038/s41550-020-01294-9
- Albert, A., Alfaro, R., Alvarez, C., et al. 2020, ApJL, 896, L29. doi:10.3847/2041-8213/ab96cc
- Amato, E. & Blasi, P. 2009, MNRAS, 392, 1591. doi:10.1111/j.1365-2966.2008.14200.x
- Arzoumanian, Z., Chernoff, D. F., & Cordes, J. M. 2002, ApJ, 568, 289. doi:10.1086/338805
- Atoyan, A. M., Aharonian, F. A., & Völk, H. J. 1995, PhRvD, 52, 3265. doi:10.1103/PhysRevD.52.3265
- Bell, A. R. 2004, MNRAS, 353, 550. doi:10.1111/j.1365-2966.2004.08097.x
- Bell, A. R., Schure, K. M., Reville, B., et al. 2013, MNRAS, 431, 415. doi:10.1093/mnras/stt179
- Blasi, P. 2013, A&A Rv, 21, 70. doi:10.1007/s00159-013-0070-7
- Caprioli, D., Haggerty, C. C., & Blasi, P. 2020, ApJ, 905, 2. doi:10.3847/1538-4357/abbe05
- Cardillo, M., Amato, E., & Blasi, P. 2015, Astroparticle Physics, 69, 1. doi:10.1016/j.astropartphys.2015.03.002
- Faucher-Giguère, C.-A. & Kaspi, V. M. 2006, ApJ, 643, 332. doi:10.1086/501516
- Ferrand, G. & Safi-Harb, S. 2012, Advances in Space Research, 49, 1313. doi:10.1016/j.asr.2012.02.004

- Fujita, Y., Bamba, A., Nobukawa, K. K., et al. 2021, arXiv:2101.10329
- Ge, C., Liu, R.-Y., Niu, S., et al. 2020, arXiv:2012.11531
- Gotthelf, E. V. & Halpern, J. P. 2007, ApJL, 664, L35. doi:10.1086/520637
- Gotthelf, E. V., Halpern, J. P., & Seward, F. D. 2005, ApJ, 627, 390. doi:10.1086/430300
- Halpern, J. P., Camilo, F., Gotthelf, E. V., et al. 2001, ApJL, 552, L125. doi:10.1086/320347
- Joncas, G. & Higgs, L. A. 1990, A&AS, 82, 113
- Kamae, T., Karlsson, N., Mizuno, T., et al. 2006, ApJ, 647, 692. doi:10.1086/505189
- Kothes, R., Uyaniker, B., & Pineault, S. 2001, ApJ, 560, 236. doi:10.1086/322511
- Leahy, D. A. & Williams, J. E. 2017, AJ, 153, 239. doi:10.3847/1538-3881/aa6af6
- Li, H. & Chen, Y. 2010, MNRAS, 409, L35. doi:10.1111/j.1745-3933.2010.00944.x
- Liu, S., Zeng, H., Xin, Y., et al. 2020, ApJL, 897, L34. doi:10.3847/2041-8213/ab9ff2
- Ohira, Y., Murase, K., & Yamazaki, R. 2011, MNRAS, 410, 1577. doi:10.1111/j.1365-2966.2010.17539.x
- Ohira, Y., Yamazaki, R., Kawanaka, N., et al. 2012, MNRAS, 427, 91. doi:10.1111/j.1365-2966.2012.21908.x
- Pineault, S. & Joncas, G. 2000, AJ, 120, 3218. doi:10.1086/316863
- Popov, S. B., Pons, J. A., Miralles, J. A., et al. 2010, MNRAS, 401, 2675. doi:10.1111/j.1365-2966.2009.15850.x
- Truelove, J. K. & McKee, C. F. 1999, ApJS, 120, 299. doi:10.1086/313176
- Xin, Y., Zeng, H., Liu, S., et al. 2019, ApJ, 885, 162. doi:10.3847/1538-4357/ab48ee
- Yuan, Q., Lin, S.-J., Fang, K., et al. 2017, PhRvD, 95, 083007. doi:10.1103/PhysRevD.95.083007
- Zavlin, V. E., Pavlov, G. G., Sanwal, D., et al. 2000, ApJL, 540, L25. doi:10.1086/312866